TR-264(1992)

Stiffness of fibre composites
- a simple approach

Lauge Fuglsang Nielsen

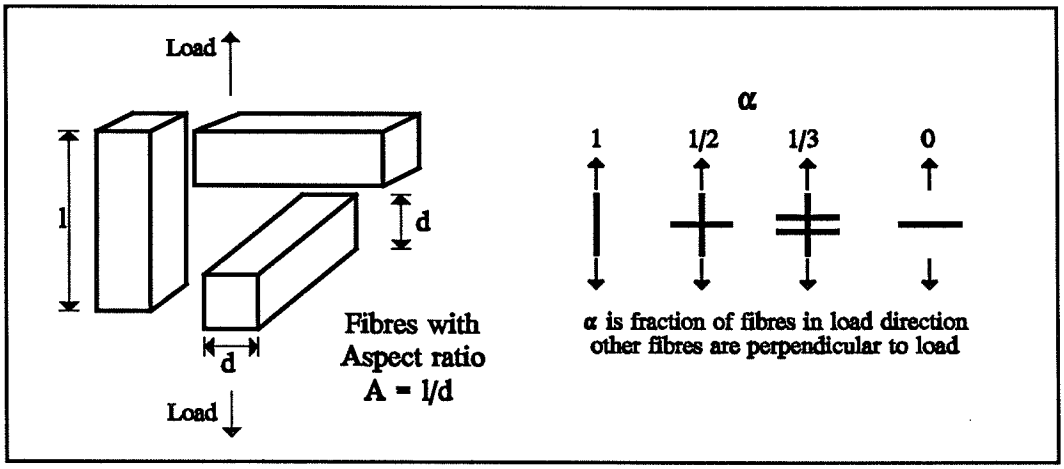

Building Materials Laboratory
Technical University of Denmark

Stiffness of fibre composites

- a simple approach

Lauge Fuglsang Nielsen
Building Materials Laboratory
Technical University of Denmark
DK-2800 Lyngby, Denmark

Content

Stiffness of fibre composites

- a simple approach

Lauge Fuglsang Nielsen
Building Materials Laboratory
Technical University of Denmark
DK-2800 Lyngby, Denmark

1. Introduction

In the past three decades considerable attention has been devoted to composite materials. A number of useful equations referenced in (1,2,3,4) for example have been suggested in the literature to predict macroscopic stiffness (elastic modulus/moduli) of composite materials from elastic properties and volume characteristics of the constituent components. Most equations are based on the very important results obtained in the early days of research in the area of composite materials:

Exact bounds for the elastic moduli of composites were developed by Paul (5) for unrestricted phase geometry and by Hashin and Shtrikman (6) for phase geometries which cause macroscopic isotropy.

Exact stiffness solutions of composites were developed for parallel layered materials by Hansen (7), for isotropic materials reinforced by spherical particles by Hashin (8), for isotropic composites with phases of equal shear moduli by Hill (9), for plane isotropic composites with parallel and very long fibres of circular cross-sections by Hashin and Rosen (10), and for plane isotropic composites with phases of equal shear moduli by Hill (11).

To date these early works still represent the only exact analysis of composites stiffness. At present, we must except that only approximate predictions of elastic moduli of real composites can be made. Real composites have geometries which can differ considerably from those theoretically considered (spheres, parallel plates, long uni-directional fibres of circular cross-sections). The influence of geometry on composites mechanical behavior is a most important subject in the analysis of composites and in design of new materials. This feature has recently been considered by the author in (3,12).

The subject of phase geometry is also dealt with in this paper. A simple self-consistent approach is used in Section 2 to illustrate the influence of distribution and aspect ratios (length/diameter) of straight fibres on the Young's modulus of some anisotropic fibre-reinforced materials modelled in Section 1.1, Figure 1. Aspect ratios considered range from 0 (penny fibres) to ∞ (very long cylindrical fibres). Special "fibre-reinforced" materials considered are porous materials and cracked materials.

Solutions obtained for parallel chopped fibre-reinforced materials are discussed relative to the Halpin-Tsai relation (13) often referred to in the literature on composite materials (e.g. 1,2,14,15,16). Solutions obtained for cubic fibre-reinforced materials are related to the

authors general theory on isotropic composites in (3). The basic material model presented and examples shown are reproduced from the author's text notes (17) on material mechanics. The terms, Young's modulus and stiffness, are synonyms in subsequent text.

1.1 Material model

Uni-axially loaded fibre-reinforced materials are considered with matrix phase S and fibre phase P. Both phases have equal Poisson's ratios. The fibres and fibre systems considered are defined in Figure 1 with quadratic straight cylinders of length l and cross-section d*d. Fibre aspect ratio is A = l/d. Orientations of fibres are parallel or perpendicular to the uniaxial load σ^* as illustrated. Fibres perpendicular to load need not have a direction of preference, meaning that thick plates (relative to fibre diameter), for example, are also considered with plane quadratic fibre arrangements. Other examples are orthotropic materials, cubic materials and plane isotropic materials with plane of isotropy perpendicular to load. Cubic fibre-reinforced materials have $\alpha = 1/3$ with fibres in the cross-load plane being perpendicular to each other. Isotropic materials are fairly well approximated by cubic models.

Parallel to load strain is $\varepsilon^* = \sigma^*/E^*$ where E^* is the unknown composite Young's modulus to be determined. Relative composite stiffness and stiffness ratio are defined by $e^* = E^*/E_S$ and $n = E_P/E_S$ respectively. Volume concentration of fibres is denoted by c (= vol of fibres/total vol of composite).

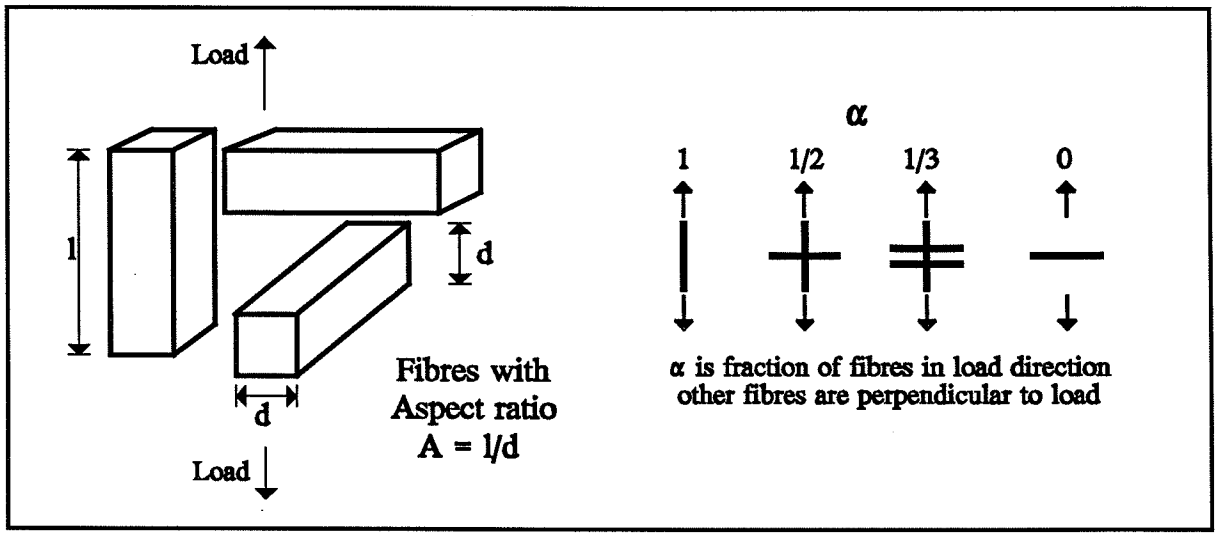

Figure 1. *Fibres and basic fibre system considered with fibres of equal lengths and aspect ratios. Fibres perpendicular to load need not have a direction of preference. Other fibre systems are present each of which is congruent with the basic system. Thus, total fibre system may consist of fibres of different lengths but constant aspect ratios.*

1.2 Max fibre concentration and voids

Increasing fibre concentration may be thought of as the result of stepwise adding small amounts of fibre systems each of which is congruent with the basic fibre system defined in Figure 1. Difficulties are met in practice using this procedure to produce tight composites with

high fibre concentrations - especially when fibres of constant lengths are used. Maximum packing of fibres forming a fixed skeleton is obtained at $c = c_{FP}$ where the latter quantity is fibre packing ratio (maximum fibre volume relative to total volume of a pile of fibres). Fibre composites with $c > c_{FP}$ can only be produced by reducing the amount of matrix. It is easily checked that the void concentration (relative to total composite volume) at $c > c_{FP}$ is expressed by Equation 1. Voids reduce stiffness in a way which can be considered approximately as shown in Section 3.13.

$$c_{VOID} = MAX\left(0, \frac{c - c_{FP}}{c}\right) \tag{1}$$

1.3 Stiffness bounds

The results developed must respect the Paul-Hansen bounds (5,7) considering composites with non-restricted geometry. In the present context these bounds can be written as shown in Equation 2, first expression. Cubic fiber systems are anticipated not to violate seriously the Hashin-Shtrikman bounds (6) applying for isotropic composites. These bounds (with Poisson's ratios 0.2) are presented in Equation 2, second expression.

$$\frac{n}{n - c(n-1)} \le e^* < 1 + c(n-1) \qquad (Anisotropy)$$
$$n\,\frac{2 + c(n-1)}{2n - c(n-1)} \le e^* < \frac{n + 1 + c(n-1)}{n + 1 - c(n-1)} \qquad \left(\begin{array}{l} Isotropy \\ reverse\ signs\ when\ n > 1 \end{array}\right) \tag{2}$$

2. Analysis

Hill (9) has shown that the remarkably simple relations shown in Equation 3 exist between averages (by volume) of stresses, strains, and stiffnesses of homogeneous (not necessarily isotropic) composite materials consisting of homogeneous and isotropically elastic components. In the present context ε, σ, and E mean strain, stress, and Young's modulus respectively in load direction. Phase considered is referred to by subscript. The expressions can be organized as shown in Equation 4 to predict composites stiffness from average stress in phase P (or to predict average stress in phase P from composites stiffness).

$$\begin{array}{l} \sigma^* = (1-c)\,\sigma_S + c\,\sigma_P \\ \varepsilon^* = (1-c)\,\varepsilon_S + c\,\varepsilon_P \end{array} \quad ; \quad \varepsilon_P = \frac{\sigma_P}{E_P} \quad ; \quad \varepsilon_S = \frac{\sigma_S}{E_S} \quad ; \quad \varepsilon^* = \frac{\sigma^*}{E^*} \tag{3}$$

$$\frac{1/e^* - 1}{1/n - 1} = c\,\frac{\sigma_P}{\sigma^*} \quad ; \quad e^* = \frac{E^*}{E_S} \quad (relative\ stiffness) \tag{4}$$

When phase P are fibres we may estimate σ_P from a single particle-infinite matrix solution replacing matrix property with the composites (not yet known) property. This means that one

of the many particles in the composite is considered separately as embedded in an infinite matrix of composite. This principle is known in composite theory (e.g. 18,19) as the "Self Consistency Scheme" (SCS).

$$\frac{\sigma_P}{\sigma^*} \approx \begin{cases} \dfrac{n(1+A)}{n+A} & \parallel \text{Cylinder} \\ \dfrac{n(1+3A)}{1+A(1+2n)} & \perp \text{Cylinder} \end{cases} \quad ; \quad \text{fibre aspect ratio } A = \frac{l}{d} \tag{5}$$

$$\frac{\sigma_P}{\sigma^*} \approx \left\{ \begin{array}{ll} \dfrac{n^*(1+A)}{n^*+A} = \dfrac{n(1+A)}{n+Ae^*} & \parallel \text{Cylinder} \\ \dfrac{n^*(1+3A)}{1+A(1+2n^*)} = \dfrac{n(1+3A)}{e^*+A(e^*+2n)} & \perp \text{Cylinder} \end{array} \right\} \quad n^* = \frac{E_P}{E^*} = \frac{n}{e^*} \tag{6}$$

The single particle solutions in Equation 5 have been developed and adapted for the current purpose by the author from Eshelby's classical analysis (20) of the stress field at an ellipsoidal particle in an infinite matrix. The multi-particles solutions presented in Equation 6 are then obtained by the SCS-approach replacing stiffness ratio n in Equation 5 with modified stiffness ratio $n^* = E_P/E^* = n/e^*$.

For the anisotropic fibre systems considered in this paper a "single" particles stress can be determined by the weighted average shown in Equation 7 where α denotes volume fraction of fibres in load direction.

$$\frac{\sigma_P}{\sigma^*} = \alpha\frac{\sigma_P}{\sigma^*}\parallel + (1-\alpha)\frac{\sigma_P}{\sigma^*}\perp \quad ; \quad (\alpha \text{ is fraction of fibres in load direction}) \tag{7}$$

2.1 Stiffness of multi-directional fiber-reinforced material

The stiffness quantities of interest are now easily obtained combining Equations 4 and 7. The results are presented in Equation 8 which in general has to be solved by numerical means. Analytical closed form solutions, however, can be obtained for some special materials such as the porous materials (n = 0), parallel fibre-reinforced materials (α = 1), and compact particle-reinforced materials (A = 1) considered in subsequent sections 3.1, 3.21, and 3.4.

$$e^* = 0.5*[M + \sqrt{M^2 + 4n/A}] \quad \text{with}$$

$$M = 1 - \frac{1}{A}\left[n + c(1-n)\left(\alpha(1+A) + (1-\alpha)\frac{(1+3A)(n+Ae^*)}{2An + (1+A)e^*}\right)\right] \tag{8}$$

3. Examples

Examples are presented in this section demonstrating the influence of fibre distribution and aspect ratio on the stiffness of fibre-reinforced materials. "Ideal" tight materials are considered primarily. Stiffness reduction due to voids is easily determined by the method presented in Section 3.13.

3.1 Porous materials (n = 0) and geometrical parameters

Equation 8 reduces as shown in Equations 9 and 10 which predict stiffness to vary linearly with porosity c. The so-called shape factor μ_o and critical concentration c_d presented in Equation 10 are important phase geometrical parameters (at any stiffness ratio n) introduced into composite analysis by the author in (3). A brief explanation is given in Section 4 on the physical meaning of μ_o and c_d. The influence of fibre aspect ratio on shape factor and critical concentration is demonstrated in Figures 2 and 3. It is observed that $\mu_o = 3/4$ is approached when cubic systems are considered with very long fibres. This quantity is close to a shape factor of $\mu_o = 0.7$ presented in (21) as a result of a FEM analysis (3) on special composite materials (CR-materials) where both phases have the geometry of perfectly fitting 3-dimensional crosses. It should be noticed that simple relationships between μ_o and c_d (such as the one presented in Equation 10) are exceptions when composite materials in general are considered, see Sections 4 and 5.

$$e^* = 1 - c\left(1 + \frac{\alpha(1 + A) + 2A^2(1 - \alpha)}{A(1 + A)}\right) \quad (\equiv 0 \text{ when predicted } e^* \leq 0) \tag{9}$$

$$e_o^* = 1 - (1 + \frac{1}{\mu_o})\, c = 1 - \frac{c}{c_d} \quad (\equiv 0 \text{ when predicted } e_o^* < 0)$$

$$\mu_o = \frac{A(1 + A)}{\alpha(1 + A) + 2A^2(1 - \alpha)} \quad \textit{(shape factor)} \tag{10}$$

$$c_d = \frac{\mu_o}{1 + \mu_o} \quad \textit{(critical concentration)}$$

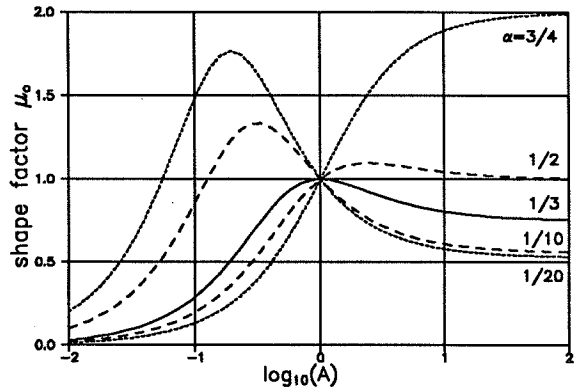

Figure 2. Shape factor μ_o for different α. Cubic fibre system has α = 1/3.

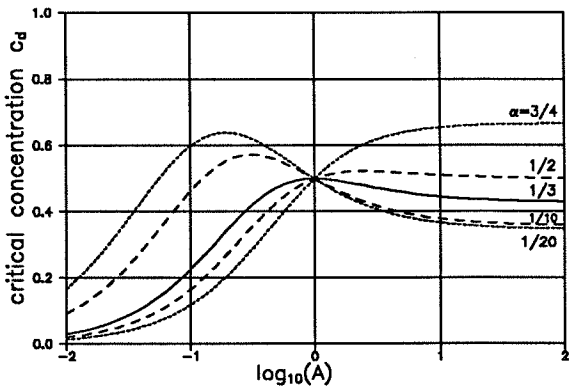

Figure 3. Critical concentration c_d for different α. Cubic system has α = 1/3.

3.11 Stiffness, pore geometry and distribution

It is noticed from Figure 2 and Equation 10 (first expression) that stiffness of porous materials with $\alpha > \approx 0.5$ will increase monotonically with increasing (fibre) pore aspect ratio. When $\alpha < \approx 0.5$ stiffness variation is not that simple. Stiffness increases monotonically with increasing aspect ratio from $A = 0$ up to a certain $A = A_{CR}$ beyond which stiffness decreases monotonically as A approaches infinity. When cubic fibre systems ($\alpha = 1/3$) are considered stiffness increases in the fibre aspect range going from $A = 0$ to $A_{CR} = 1$, while it decreases going from $A_{CR} = 1$ to $A = \infty$. Stiffness of systems with $\alpha = 0$ will always decrease with increasing fibre aspect ration because $A_{CR} = 0$.

3.12 Cracked material (n = 0, A → 0)

Cracked materials are porous materials with a vanishing pore aspect ratio, meaning that porosity $c = pld^2 = pAd^3$ is introduced into Equation 10 together with $A \rightarrow 0$. Crack density p is number of cracks per volume unit. The result is presented in Equation 11 and Figure 4. (Strength of cracked and porous materials has recently been considered by the author in (22), see also (23). Strength in general of fibre-reinforced materials is considered in special literature on this subject (e.g. 1,24,25,26,27,28)).

$$e^* = 1 - p\alpha d^3 \quad \textit{with crack density } p \tag{11}$$

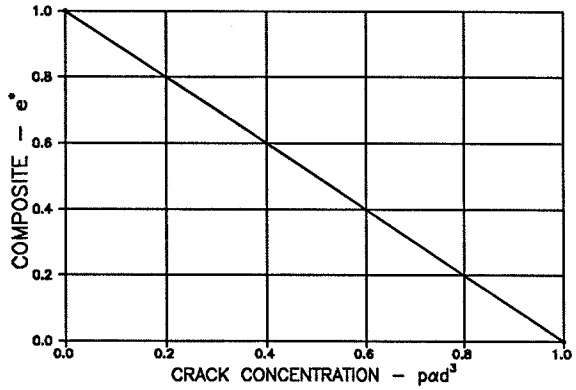

Figure 4. *Stiffness of material with orthotropic crack system. Crack density is p (number of cracks per vol-unit). Cubic systems have* $\alpha = 1/3$.

$$e^*_{RED}(c) = e^*_o(c_{VOID}) * e^*(c) \quad ; \quad e^*_o(c_{VOID}) = \begin{cases} 1 & c \le c_{FP} \\ MAX\left[\dfrac{(1+\mu_o)c_{FP} - c}{\mu_o c}, 0\right] & c > c_{FP} \end{cases} \tag{12}$$

In subsequent text is assumed: $c_{FP} \approx c_d$

3.13 Stiffness reduction due to voids

It has been mentioned in Section 1.2 that tight fibre composites are impossible to produce with fibre concentrations greater than the fibre packing ratio c_{FP}. Voids are inevitable. The stiffness reduction due to this phenomenon can be determined approximately as suggested in (3,29) and reproduced by the first expression in Equation 12. Reduced modulus is e^*_{RED}. "No voids" stiffness is $e^*(c)$ (Equation 8). Reduction factor $e^*_o(c_{VOID})$ is stiffness of porous material

(Equation 10) at porosity c_{VOID} (Equation 1). Subscript "RED" is not used in the following text as the proper meanings of the e^*-quantities presented are quite obvious.

3.2 Parallel fibre-reinforced material

3.21 Parallel to load ($\alpha = 1$)

The M factor in Equation 8 reduces as shown in Equation 13. Examples of stiffness predictions are presented in Figures 5 and 6. Also shown in the figures are the anisotropic (P/H) bounds from Equation 2.

$$M = n(1 - 1/A) + (1 - n)[1 - c(1 + 1/A)] \quad (13)$$

3.22 Perpendicular to load ($\alpha = 0$)

The results shown in Figures 7 and 8 are composite Young's moduli of systems where all fibres are perpendicular to load. Also shown in the figures are the anisotropic (P/H) bounds from Equation 2.

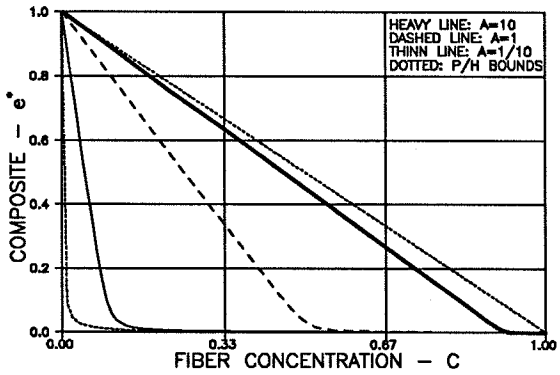

Figure 5. Stiffness of uni-directional fibre system ($\alpha = 1$). Stiffness ratio $n = 0.001$.

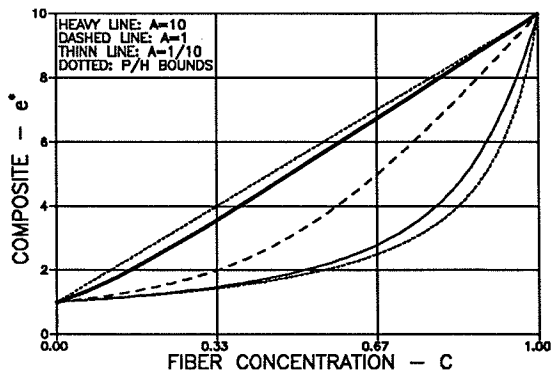

Figure 6. Stiffness of uni-directional fibre system ($\alpha = 1$). Stiffness ratio $n = 10$.

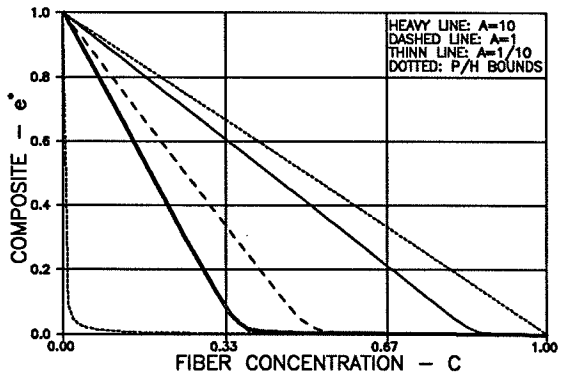

Figure 7. Stiffness perpendicular to one or two-dimensional fiber systems. No fibres in load direction ($\alpha = 0$). Stiffness ratio is $n = 0.001$.

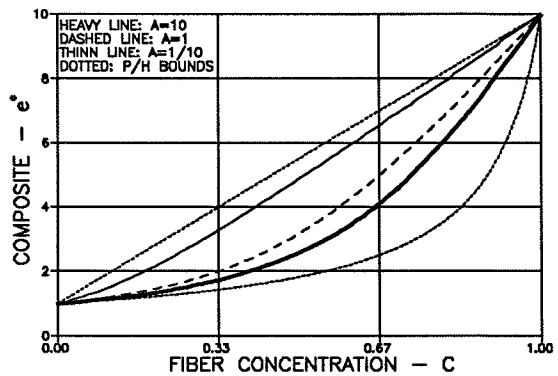

Figure 8. Stiffness perpendicular to one or two-dimensional fiber systems. No fibres in load direction ($\alpha = 0$). Stiffness ratio is $n = 10$.

It is noticed from Figures 5 - 8 that predicted stiffness does not violate the anisotropic bounds from Equation 2 (first expression). It is further noticed from Figures 5 and 7 that shorter fibres reduce stiffness along the fibres and increase stiffness perpendicular to fibres respectively in uni-directional fibre systems made with soft fibres (n << 1). This observation agrees with the comments made in Section 3.11 on stiffness of porous materials as related to pore geometry. A similar trend is observed from Figures 6 and 8 when fibres are stiff (n >> 1).

3.3 Cubic fibre-reinforced materials a.o. (α = 1/3)

Figures 9 and 10 refer to systems where 2/3 of the fibres are perpendicular to load (α = 1/3). The isotropic bounds from Equation 2, second expression, are also shown in these figures.

It is noticed that predicted stiffness of a cubic fibre system does not violate seriously the isotropic bounds. It is further noticed from Figure 9 that stiffness is decreased for soft fibre-reinforced materials both when shorter (A < 1) and longer (A > 1) fibres are used. This observation agrees with the comments made in Section 3.11 on stiffness of porous materials versus pore geometry. The trend of stiffness variation just observed for soft fibres is reversed, as can be seen from Figure 10, when stiff fibre-reinforced materials are considered.

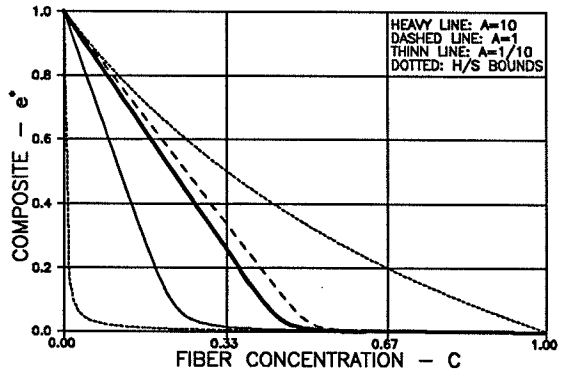

Figure 9. Stiffness in fibre direction x of fibre system with 67 % fibres perpendicular to x (α = 1/3). Stiffness ratio n = 0.001.

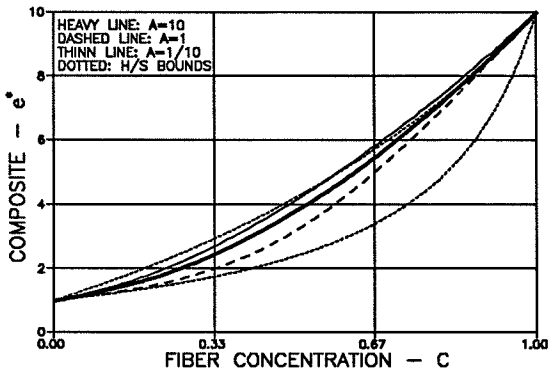

Figure 10. Stiffness in fibre direction x of fibre system with 67 % fibres perpendicular to x (α = 1/3). Stiffness ratio n = 10.

3.4 Compact particle-reinforced material (A = 1)

Equation 8 reduces for any α as shown in Equation 14 which is identical to an expression which can be be obtained from Budiansky's analysis (19) on isotropic composites made by compaction of powders of compact shapes.

$$e^* = \frac{1}{2}[(1 - n)(1 - 2c) + \sqrt{(1 - n)^2(1 - 2c)^2 + 4n}\ ] \qquad (14)$$

4. Isotropic composite materials

Equation 15 has been developed by the author (3,12,21) to predict stiffness of isotropic composite materials with arbitrary phase geometry.

Shape factor μ_o and critical volume concentration c_d are parameters which characterize the geometrical complexity of phase P (discrete, continuous, or mixed) at low concentrations and interaction between phase elements at higher concentrations respectively. Spherical shapes have the maximum shape factor of $\mu_o = 1$. Shape factors decrease with increasing shape complexity (away from spheres, higher specific surfaces). Phase elements like crumbled sheets have shape factors close to the minimum of $\mu_o = 0$. Estimates on shape factors versus phase geometry are given in (3,12).

$$e^* = \frac{n + \theta[1 + c(n-1)]}{n + \theta - c(n-1)} \quad \textit{with}$$

$$\theta = 0.5[\mu + n\mu' + \sqrt{(\mu + n\mu')^2 + 4n(1 - \mu - \mu')}\,] \quad \textit{Geometry function} \qquad (15)$$

$$\mu = \mu_o \frac{c_d - c}{c_d} \;;\; \mu' = MIN\left(\mu_o \frac{c - c_D}{c_d},\, 1\right) \quad \textit{Shape functions}$$

Critical concentration c_d is concentration where phase P dissolves phase S into discrete particles. Extremely well graded phase P particles (maintaining their low porosity shapes) have high critical volume concentration ($c_d > 1$). Badly graded particles (increasing particles agglomeration at increasing concentration) have lower critical concentrations ($c_d < 1$). Thus, the size of c_d is very much a matter of fabrication technique. No fixed correlation exists between μ_o and c_d when real composite materials are considered. (Critical concentration c_D is concentration where phase P leaves the state of being fully discrete).

The isotropic bounds in Equation 2 are predicted by Equation 15 introducing $\theta \equiv 1$ and $\theta \equiv n$ respectively which according to (3) correspond to spheres ($\mu_o = 1$) of phase P in a continuous phase S ($c_d = \infty$) and phase S spheres in a continuous phase P ($c_D = -\infty$) respectively.

4.1 Porous Materials

Equation 15 reduces as shown in Equation 16 when porous materials are considered with $n = 0$.

$$e^* = \theta\frac{1 - c}{\theta + c}$$

$$e^* \to 1 - (1 + \frac{1}{\mu_o})c \quad \textit{when } c \to 0 \qquad (16)$$

$$\theta = \mu_o(1 - c/c_d) \quad \textit{Geometry function } (\equiv 0 \textit{ when } \theta < 0 \textit{ is predicted})$$

4.2 Fibre-reinforced materials

The shape factor μ_o and critical concentration c_d suggested in Equation 17 for isotropic fibre-reinforced materials are suggested from Equations 10 with $\alpha = 1/3$. The critical concentration c_D is an estimate based on numerical calculations comparing Equations 8 and 15. Examples of predicting the stiffness of isotropic fibre-reinforced materials by Equation 15 with geometrical parameters from Equation 17 are shown in Figures 11 and 12 which do not

deviate very much from Figures 9 and 10 which represent the cubic results of the analysis developed in Section 2 of this paper.

$$\mu_o = \frac{3A(1+A)}{1+A+4A^2} \quad ; \quad c_d = \frac{\mu_o}{1+\mu_o} \quad ; \quad c_D = \frac{(2c_d)^{10}}{2} \tag{17}$$

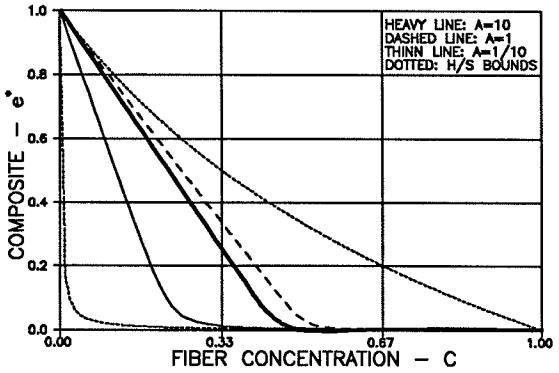

Figure 11. Isotropic fibre system with μ_o, c_d, c_D from Equation 17 and n = 0.001.

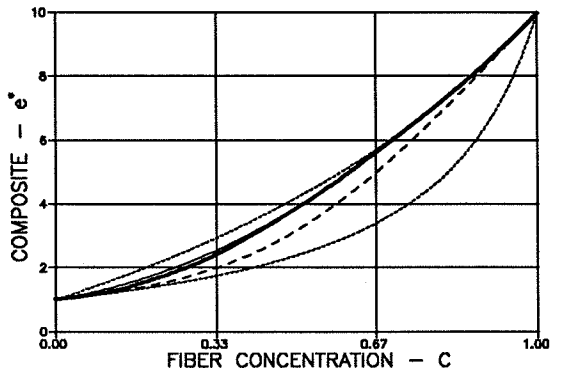

Figure 12. Isotropic fibre system with μ_o, c_d, c_D from Equation 17 and n = 10.

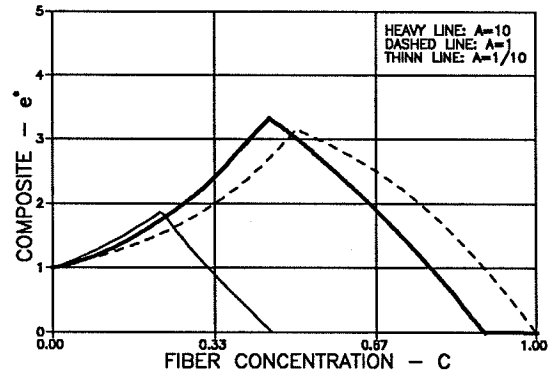

Figure 13. Isotropic fibre system. Equation 15 with μ_o, c_d, c_D from Equation 17 and n = 10. Stiffness reduction from Equation 12.

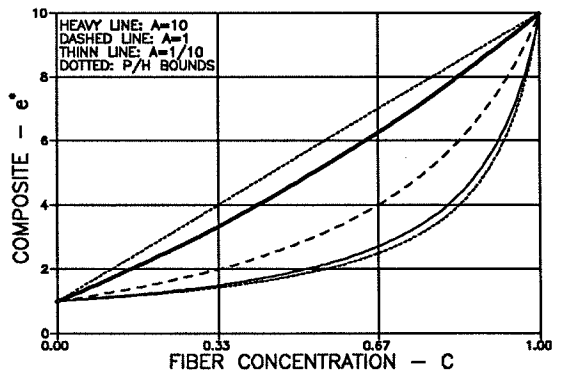

Figure 14. Stiffness parallel to uni-directional fibre system (α = 1) predicted by Halpin-Tsai's expression. n = 10.

4.3 Special observations on isotropy/anisotropy

It is noticed that the anisotropic lower and upper bounds in Equation 2 are described by Equation 15 with $\theta \equiv 0$ and $\theta \equiv \infty$ respectively. This feature indicates that it might be worthwhile exploring the possibilities of generalizing Equation 15 also to consider anisotropic composites. A first attempt of generalization might be to introduce a geometry function $\theta = 2A^{(3\alpha-1)/2}$ into Equation 15. Immediate consequences of this approach are the following:

Stiffness perpendicular to unidirectional fibre system ($\alpha = 0$, $\theta = 2A^{-1/2}$): Upper and lower anisotropic bounds from Equation 2 are approached as $A \to 0$ and $A \to \infty$ respectively.

Stiffness in one fibre direction of qubic fibre system: ($\alpha = 1/3$, $\theta = 2$): Stiffness is predicted independent of fibre aspect ratio.

Stiffness parallel to unidirectional fibre system ($\alpha = 1$, $\theta = 2A$): Upper and lower anisotropic bounds from Equation 2 are approached as $A \rightarrow \infty$ and $A \rightarrow 0$ respectively.

Trend evaluation and order of magnitudes comparison between results obtained by the "model" outlined above ($\theta = 2A^{(3\alpha-1)/2}$ in Equation 15) and the results obtained by Equation 8 in Section 2 show that the model might serve as a qualified basis of developing a proper and more detailed generalization (also considering the stiffness ratio) of Equation 15 with more accurate answers (for example, with respect to the stiffness influence of aspect ratio at $\alpha = 1/3$).

It is of interest to notice that the Halpin-Tsai (H/T) expression (13) often used in practice to predict parallel to fibre stiffness of uni-directional fibre systems complies well with the model considered. The H/T expression can be re-formulated as Equation 15 with $\theta \equiv 2A$. Examples of H/T stiffness predictions are shown in Figure 14.

5. Conclusions and final remarks

Young's moduli of some anisotropic fibre composites have been predicted by a method developed in Section 2 and examplified in Section 3. The results obtained are admissible. They do not violate the anisotropic bounds given in Equation 2. The anisotropic upper bound stiffness is approached with very long fibres parallel to load ($\alpha = 1$, $A \rightarrow \infty$). Stiffness quantities predicted for cubic fiber systems ($\alpha = 1/3$) do not violate seriously the isotropic bounds given in Equation 2 which indicates that stiffness of isotropic fibre systems can be predicted reasonably well by the cubic expressions presented in the paper. When fibres are compact particles ($A = 1$) stiffness results are predicted which are identical to results which can be obtained from an analysis in (19) on composites made of compacted powders. Stiffness moduli parallel to fibres in uni-directional fibre systems are obtained (Figure 6) which compare positively with results predicted by the Halpin-Tsai expression (13), Figure 14.

Composite stiffness is significantly and systematically influenced by fibre geometry (orientation and aspect ratio). This feature is discussed in details in Sections 3.11, 3.2 and 3.3.

The results obtained for cubic fibre systems are used in Section 4 to suggest how the stiffness of real isotropic fibre systems can be predicted by a more general theory of isotropic composites previously developed by the author. The general theory is more flexible with respect to critical concentration (c_d) which defines interaction between fibres in real fibre systems. A further advantage offered by the general theory is that the effect of not-straight and twisted fibres on stiffness can be considered with lower (experimentally deduced) quantities of shape factor μ_o and c_d than what is predefined by the theoretical analysis presented in Section 2.

A discussion is made in Section 4.3 on geometrical relationships between the methods presented in the paper on stiffness prediction of anisotropic fibre-reinforced materials and on isotropic composite materials respectively. A possible link between the two methods is identified. It is shown, for example, how the Halpin/Tsai expression previously referred to can be "predicted" by the isotropic theory presented.

A subsequent paper deals with viscoelastic properties, shrinkage, thermal expansion, and thermal and electric conductivity of fibre reinforced materials.

Literature

1. Broutman, L.J., and Krock, R.H. (eds): "Composite Materials, Vol. 2: Mechanics of Composite Materials", Academic Press, New York, 1974.

2. Hale, F.K.: "The physical properties of composite materials". J. Mater. Sci., 11(1976), 2105.

3. Nielsen, L. Fuglsang: "Elastic properties of two-phase materials". Mat. Sc. and Eng., 1982, 39-62

4. Holliday, L.(ed): "Composite materials", Elsevier Publishing Comp., Amsterdam 1966.

5. Paul, B.: "Prediction of elastic constants of multi-phase materials". Trans. of the Metallurgical Soc. of AIME, 218(1960), 36 - 41.

6. Hashin, Z. and Shtrikman, S.: "Variational approach to the theory of elastic behavior of multi-phase materials". J. Mech. Solids, 11(1963), 127 - 140.

7. Hansen, T.C.: "Creep of concrete: A discussion of some fundamental problems". Bulletin no. 33(1958), Svenska Forskningsinstitutet för Cement och Betong, Tekniska Högskolan, Stockholm".

8. Hashin, Z.: "Elastic moduli of heterogeneous materials". J. Appl. Mech., 29 (1962), 143 - 150.

9. Hill, R.: "Elastic properties of reinforced solids: Some theoretical principles". J. Mech. Phys. Solids, 11(1963), 357 - 372.

10. Hashin, Z. and Rosen, B.W.: J. Appl. Mech., 31(1964), 223.

11. Hill, R.: J. Mech. Phys. Solids, 12(1964), 199.

12. Nielsen, L. Fuglsang: "Elasticity and damping of porous and impregnated materials". Journ. Am. Ceramic Soc., 1984, 93-98.

13. Halpin, J.C.: Journ. Composite Materials, 3(1969), 732.

14. Chow, T.S.: "The effect of particle shape on the mechanical properties of filled polymers", Journ. Materials Science, 15(1980), 1873 - 1888.

15. Halpin, J.C. and N.J. Pagano: "Stiffness and Expansion Estimates for oriented and random fibrous composites". AFML-TR-69-341, 1970.

16. Jenness Jr., J.R. and D.E. Kline: "Dynamic mechanical properties of some epoxy matrix composites", Journ. Appl. Polymer Science, 17(1973), 3391-3422.

17. Nielsen, L. Fuglsang: "Materialemekanik II - Rheologi, brud, kompositmaterialer og levetid", (Text notes in danish, Material mechanics - rheology, failure, composite materials, and lifetime), Build. Mat. Lab., Tech. Univ. Denmark, tech. report 189(1988).

18. Böttcher, C.J.F.: Rec. Trav. Chim. Pays-Bas, 64(1945), 47.

19. Budiansky, B.: On the elastic moduli of some heterogeneous materials". J. Mech. Phys. Solids, 13(1965), 223 - 227.

20. Eshelby, J.D.: "The determination of the elastic field of an ellipsoidal inclusion, and related problems", Proc. R. Soc. London, Ser. A, 241(1957), 376- 396.

21. Nielsen, L. Fuglsang: "Shrinkage, swelling, and stiffness of composites - strain and stress caused by hygro-thermal action and solidification or freezing of liquid impregnant", Bygningsstatiske Meddelelser, Denmark, 62(1991), 47-78.

22. Nielsen, L. Fuglsang: "Strength and stiffness of porous materials", Journ. Am. Ceramic Soc. 73(1990), 2684-89.

23. Bache, H.H.: "Development of Materials on basis of fracture mechanics", Dansk Beton, 2(1990), 64-70.

24. Krenchel, H.: "Fibre reinforcement", thesis, Akademisk Forlag, Copenhagen, 1964.

25. Dharan, C.K.H.: Fracture mechanics of composite materials", J. Eng. Mat. Tech., 100(1978), 233-347.

26. Sih, G.C. and A.M. Skudra (eds): "Failure mechanics of composites", Vol. 3, 1985, in A. Kelly and Yu. N. Rabotnov (eds): "Handbook of composites", Vol. 1-4, North Holland, Elsevier Science Publishers, Amsterdam.

27. Stang, H.: "Strength of composite materials with small cracks in the matrix", Int. J. Solids Structures, 22(1986), 1259-1277.

28. Stang, H,: "A double inclusion model for microcrack arrest in fibre reinforced brittle materials", J. Mech. Phys. Solids, 35(1987), 325-342.

29. Nielsen, L. Fuglsang: "Elastizitätsmodul der Kompositmateriale insbesondere Mörtel und Beton" (in german, Young's modulus of composite materials - with special relevance to mortar and concrete). Acta Polytechnica Scandinavica, Physics including Nucleonic Series No. 65(1970).